Syndiotatic Polystyrene Aerogels with β, γ, and ε Crystalline Phases

Christophe Daniel,* Simona Giudice, and Gaetano Guerra

Dipartimento di Chimica and INSTM Research Unit, Università di Salerno, Via Ponte Don Melillo, 84084 Fisciano, Italy

Received September 18, 2008. Revised Manuscript Received November 18, 2008

The influence of thermal treatments and supercritical carbon dioxide extraction procedures on the crystal structure and morphology of sPS aerogels is investigated mainly by wide-angle X-ray diffraction and scanning electron microscopy. The use of supercritical CO_2 extraction treatments allows the obtaining of high porosity aerogels with fibrillar morphology, not only exhibiting the nanoporous δ phase but also the dense γ and β crystalline phases. Moreover, a procedure to obtain high-porosity aerogels exhibiting the recently discovered nanoporous ε-form is described. Measurements of the sorption capacity of organic molecules from diluted aqueous solutions, for aerogels presenting different crystalline phases, clearly indicate that ε-form aerogels are the only ones suitable for detection and removal of long organic pollutants.

Introduction

It has been shown recently that high-porosity sPS aerogels can be obtained by supercritical CO_2 extraction of the solvent present in sPS physical gels[1a,b] or by sublimation of the solvent.[1c,d] The crystalline phase of the aerogels as well as their structure depend on the crystalline structure (cocrystalline or β) of the junction zones of the starting gel.[1a,b] Elastic gels for which the polymer-rich phase is a cocrystal phase[2] are obtained with low-molecular-mass guest molecules[3] (also called type I gels[3g]) and the corresponding aerogels are formed by semicrystalline nanofibrils (fibril diameter range between 30−200 nm) exhibiting the nanoporous crystalline δ-form.[4] With bulky solvent molecules unable to form sPS cocrystals, pastelike solids with much lower elasticity for which the crystalline phase is the thermodynamically stable and dense β-form[5] can be obtained[6] (also called type II gels[3g]) and the corresponding aerogels are characterized by β-form interconnected lamellar crystals (thickness in the range 200−400 nm).[1a,b]

Sorption measurements of volatile organic compounds (VOC) have shown that sPS δ-form aerogels exhibit a much higher sorption capacity of VOC (both from vapor phase and from dilute aqueous solutions) than sPS aerogels with dense crystalline phases.[1e] The high VOC sorption capacity of δ-form aerogels is similar to those observed with other δ-form samples (i.e., film or powder)[7] but the VOC diffusivity in the aerogel from water solutions is several orders faster than in film samples.[1e] The sorption properties of

* Corresponding author. E-mail: cdaniel@unisa.it.

(1) (a) Daniel, C.; Alfano, D.; Venditto, V.; Cardea, S.; Reverchon, E.; Larobina, D.; Mensitieri, G.; Guerra, G. *Adv. Mater.* **2005**, *17*, 1515–1518. (b) Guerra, G.; Mensitieri, G.; Venditto, V.; Reverchon, E.; Daniel, C. PCT Int. Appl. WO 2005012402, 2005. (c) Malik, S.; Rochas, C.; Guenet, J.-M. *Macromolecules* **2005**, *38*, 4888–4893. (d) Malik, S.; Roizard, D.; Guenet, J.-M. *Macromolecules* **2006**, *39*, 5957–5959. (e) Daniel, C.; Sannino, D.; Guerra, G. *Chem. Mater.* **2008**, *20*, 577–582.

(2) (a) Chatani, Y.; Inagaki, T.; Shimane, Y.; Ijitsu, T.; Yukimori, T.; Shikuma, H. *Polymer* **1993**, *34*, 1620–1624. (b) Chatani, Y.; Inagaki, T.; Shimane, Y.; Shikuma, H. *Polymer* **1993**, *34*, 4841–4845. (c) De Rosa, C.; Rizzo, P.; Ruiz de Ballesteros, O.; Petraccone, V.; Guerra, G. *Polymer* **1999**, *40*, 2103–2110. (d) Petraccone, V.; Tarallo, O.; Venditto, V.; Guerra, G. *Macromolecules* **2005**, *38*, 6965–6971. (e) Tarallo, O.; Petraccone, V.; Venditto, V.; Guerra, G. *Polymer* **2006**, *47*, 2402–2410.

(3) (a) Kobayashi, M.; Nakaoki, T.; Ishihara, N. *Macromolecules* **1990**, *23*, 78–83. (b) Kobayashi, M.; Kosaza, T. *Appl. Spectrosc.* **1993**, *9*, 1417–1424. (c) Deberdt, F.; Berghmans, H. *Polymer* **1993**, *34*, 2192–2201. (d) Daniel, C.; Dammer, C.; Guenet, J. M. *Polymer* **1994**, *35*, 4243–4246. (e) Kobayashi, M.; Yoshioka, T.; Kozasa, T.; Tashiro, K.; Suzuki, J.-I.; Funahashi, S.; Izumi, Y. *Macromolecules* **1994**, *27*, 1349–1354. (f) Daniel, C.; Deluca, M. D.; Guenet, J. M.; Brulet, A.; Menelle, A. *Polymer* **1996**, *37*, 1273–1280. (g) Roels, T.; Deberdt, F.; Berghmans, H. *Prog. Colloid Polym. Sci.* **1996**, *102*, 82–85. (h) Daniel, C.; Menelle, A.; Brulet, A.; Guenet, J.-M. *Polymer* **1997**, *38*, 4193–4199. (i) Rastogi, S.; Goossens, J. G. P.; Lemstra, P. J. *Macromolecules* **1998**, *31*, 2983–2998. (j) Daniel, C.; Musto, P.; Guerra, G. *Macromolecules* **2002**, *35*, 2243–2251. (k) Van Hooy-Corstjens, C. S. J.; Magusin, P.C. M.; Rastogi, S.; Lemstra, P. J. *Macromolecules* **2002**, *35*, 6630–6637. (l) Daniel, C.; Alfano, D.; Guerra, G.; Musto, P. *Macromolecules* **2003**, *36*, 5742–5750. (m) Shimizu, H.; Wakayama, T.; Wada, R.; Okabe, M.; Tanaka, F. *Polym. J.* **2005**, *37*, 294–298. (n) Malik, S.; Rochas, C.; Guenet, J. M. *Macromolecules* **2006**, *39*, 1000–1007.

(4) (a) De Rosa, C.; Guerra, G.; Petraccone, V.; Pirozzi, B. *Macromolecules* **1997**, *30*, 4147–4152. (b) Milano, G.; Venditto, V.; Guerra, G.; Cavallo, L.; Ciambelli, P.; Sannino, D. *Chem. Mater.* **2001**, *13*, 1506–1511. (c) Sivakumar, M.; Mahesh, K. P. O.; Yamamoto, Y.; Yoshimizu, H.; Tsujita, Y. *J. Polym. Sci., Part B: Polym. Phys.* **2005**, *43*, 1873–1880.

(5) (a) De Rosa, C.; Rapacciuolo, M.; Guerra, G.; Petraccone, V.; Corradini, P. *Polymer* **1992**, *33*, 1423. (b) Chatani, Y.; Shimane, Y.; Ijitsu, T.; Yukinari, T. *Polymer* **1993**, *34*, 1625.

(6) (a) Li, Y.; Xue, G. *Macromol. Rapid Commun.* **1998**, *19*, 549–552. (b) Daniel, C.; Alfano, D.; Guerra, G.; Musto, P. *Macromolecules* **2003**, *36*, 1713–1716.

(7) (a) Manfredi, C.; Del Nobile, M. A.; Mensitieri, G.; Guerra, G.; Rapacciuolo, M. *J. Polym. Sci., Polym. Phys. Ed.* **1997**, *35*, 133–140. (b) Musto, P.; Manzari, M.; Guerra, G. *Macromolecules* **1999**, *32*, 2770–2776. (c) Guerra, G.; Milano, G.; Venditto, V.; Musto, P.; De Rosa, C.; Cavallo, L. *Chem. Mater.* **2000**, *12*, 363–368. (d) Musto, P.; Mensitieri, G.; Cotugno, S.; Guerra, G.; Venditto, V. *Macromolecules* **2002**, *35*, 2296–2304. (e) Yamamoto, Y.; Kishi, M.; Amutharani, D.; Sivakumar, M.; Tsujita, Y.; Yoshimizu, H. *Polym. J.* **2003**, *35*, 465–469. (f) Saitoh, A.; Amutharani, D.; Yamamoto, Y.; Tsujita, Y.; Yoshimizu, H.; Okamoto, S. *Polym. J.* **2003**, *35*, 868–873. (g) Mensitieri, G.; Venditto, V.; Guerra, G. *Sens. Actuators, B* **2003**, *92*, 255–261. (h) Larobina, D.; Sanguigno, L.; Venditto, V.; Guerra, G.; Mensitieri, G. *Polymer* **2004**, *45*, 429–436. (i) Giordano, M.; Russo, M.; Cusano, A.; Mensitieri, G.; Guerra, G. *Sens. Actuators, B* **2005**, *109*, 177–184. (j) Venditto, V.; De Girolamo Del Mauro, A.; Mensitieri, G.; Milano, G.; Musto, P.; Rizzo, P.; Guerra, G. *Chem. Mater.* **2006**, *18*, 2205–2210.

10.1021/cm802537g CCC: $40.75
Published on Web 02/06/2009

δ-form aerogels associated with convenient handling characteristics makes these materials particularly interesting for applications in water and moist air purification.

Recently, a second nanoporous crystalline form of sPS named ε, has been discovered.[8] This new crystalline phase is characterized by channel-shaped cavities crossing the unit cells along the *c* axis,[8] rather than by isolated cavities as observed for the δ-form.[4a,b] This different type of nanoporosity generally leads to an orientation of the guest molecular planes parallel to the polymer host chain axes, in cocrystals obtained from the ε-phase[8] rather than perpendicular, as generally observed[2,9] for cocrystals from the δ-phase. Moreover, the ε-phase channels allow us to obtain cocrystals with guest molecules much longer than those hosted by the δ "polymeric framework".[8a]

In this contribution, for sPS gels exhibiting cocrystalline phases, the influence of thermal treatments and supercritical carbon dioxide extraction temperature on the morphology, the porosity, and the crystalline structure of the obtained aerogels will be investigated. Moreover, a procedure to obtain high-porosity aerogels with the new nanoporous crystalline ε-form will be described, and results about the sorption capacity of organic compounds from diluted aqueous solutions for aerogels exhibiting similar and high porosity but different crystalline phases will be presented.

Experimental Section

Materials. The syndiotactic polystyrene used in this study was manufactured by Dow Chemicals under the trademark Questra 101. ^{13}C nuclear magnetic resonance characterization showed that the content of syndiotactic triads was over 98%. The mass average molar mass obtained by gel permeation chromotography (GPC) in trichlorobenzene at 135 °C was found to be $M_w = 3.2 \times 10^5$ g mol^{-1} with a polydispersity index $M_w/M_n = 3.9$. Solvents used to prepare the gels were purchased from Aldrich and used without further purification.

All sPS gel samples were prepared in hermetically sealed test tubes by heating the mixtures above the boiling point of the solvent until complete dissolution of the polymer and the appearance of a transparent and homogeneous solution had occurred. The hot solution was then cooled to room temperature, where gelation occurred.

δ-Form aerogels were obtained by treating sPS gels with a SFX 200 supercritical carbon dioxide extractor (ISCO Inc.) using the following conditions: $T = 40$ °C, $P = 200$ bar, extraction time $t = 60$ min.

With the same apparatus, γ-form sPS aerogels were obtained by treating gels using the following conditions: $T = 130$ °C, $P = 200$ bar, extraction time $t = 120$ min, whereas the β-form aerogels were obtained using the following conditions: $T = 150$ °C, $P = 200$ bar, extraction time $t = 120$ min.

The porosity *P* of aerogel samples can be expressed as a function of the aerogel apparent density ρ_a as

$$P = 100\left(1 - \frac{\rho_a}{\rho_S}\right)$$

where ρ_S is the skeletal density of the polymer (e.g., equal to 1.02 and 1.06 g/cm^3 for semicrystalline sPS samples with a crystallinity of 40%, exhibiting δ- and β-phases, respectively).

Techniques. X-ray diffraction patterns were obtained on a Phillips PW1710 automatic diffractometer operating with a nickel-filtered Cu Kα radiation.

The degree of crystallinity of the aerogels was evaluated from X-ray diffraction data applying the standard procedure of resolving the diffraction pattern into two areas corresponding to the contributions of the crystalline and amorphous fractions.

Evaluation of the correlation length *D* of the crystalline domains (where an ordered disposition of the atoms is maintained) was effected using the Scherrer formula

$$D = 0.9\lambda/(\beta\cos\theta)$$

where β is the full width at half-maximum expressed in radians, λ the wavelength, and θ the diffraction angle. The value of β was corrected from the experimental effects applying the procedure described in ref 10. In particular, a KBr powder sample having a full width at half-maximum of 0.17°, under the same geometrical conditions, was used.

Thermogravimetric measurements (TGA) were performed with a TG 209 F1 from Netzsch.

Aerogel equilibrium sorption uptakes with aqueous solutions were obtained by measurements of FTIR absorbances of conformationally sensitive peaks of 1,2-dichloroethane (DCE),[11] by using calibration curves analogous to those described in refs.[11,3j,l]

Infrared spectra were obtained at a resolution of 2.0 cm^{-1} with Bruker spectrometers (Vertex70 and Tensor27) equipped with deuterated triglycine sulfate (DTGS) detector and a KBr beam splitter. The frequency scale was internally calibrated to 0.01 cm^{-1} using a He−Ne laser. 32 scans were signal averaged to reduce the noise.

Scanning electron micrographs were obtained using a Leica 440 scanning electron microscope.

Surface areas were obtained by N_2 adsorption measurements carried out at 77K on a Micromeritics ASAP 2020 sorption analyzer.

Results and Discussion

(A) Low-Porosity γ- and α-Form Aerogels by Thermal Treatment of δ-Form Aerogels. The X-ray diffraction pattern of a δ-form aerogel obtained by supercritical CO_2 extraction of a gel prepared in DCE at $C_{pol} = 5$ wt % (analogous to those shown in previous reports)[1a,b] is shown in Figure 1a. The X-ray diffraction patterns of this aerogel after annealing at 130 and 220 °C are also shown in Figure 1 (curves b and c, respectively). Similar X-ray diffraction patterns are observed for aerogels obtained by the same extraction and annealing procedures from toluene-based gels.

The X-ray diffraction pattern of the aerogel annealed at 130 °C (Figure 1b) displays strong reflections at $2\theta = 9.3$, 10.4, 16, and 20.1°, clearly showing the formation of the γ-form,[13] whereas the reflections at $2\theta = 6.7$, 11.7, 13.3,

(8) (a) Rizzo, P.; Daniel, C.; De Girolamo Del Mauro, A.; Guerra, G. *Chem. Mater.* **2007**, *19*, 3864–3866. (b) Rizzo, P.; D'Aniello, C.; De Girolamo Del Mauro, A.; Guerra, G. *Macromolecules* **2007**, *40*, 9470–9474. (c) Petraccone, V.; Ruiz de Ballesteros, O.; Tarallo, O.; Rizzo, P.; Guerra, G. *Chem. Mater.* **2008**, *20*, 3663–3668.

(9) (a) Albunia, A. R.; Milano, G.; Venditto, V.; Guerra, G. *J. Am. Chem. Soc.* **2005**, *127*, 13114–13115. (b) Daniel, C.; Galdi, N.; Montefusco, T.; Guerra, G. *Chem. Mater.* **2007**, *19*, 3302–3308.

(10) Klug, H. P.; Alexander, L. E. In *X-ray Diffraction Procedure*; John Wiley: New York, 1959; Chapter 9.

(11) Guerra, G.; Manfredi, C.; Musto, P.; Tavone, S. *Macromolecules* **1998**, *31*, 1329–1334.

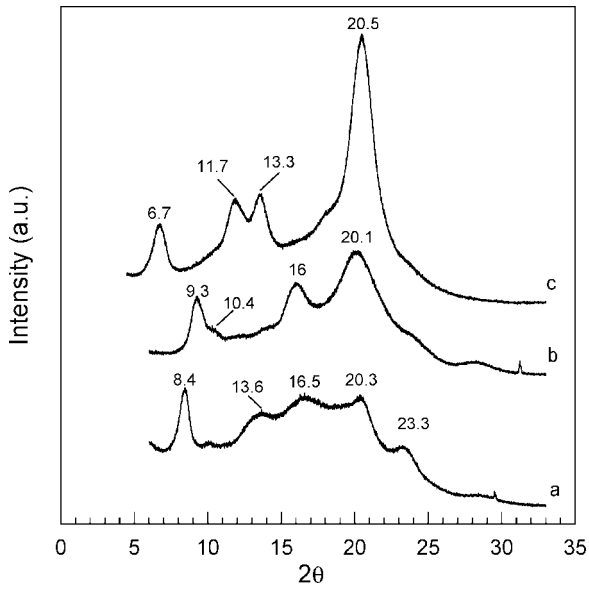

Figure 1. X-ray diffraction patterns of sPS aerogels: (a) obtained by supercritical carbon dioxide extraction at 40 °C of gels prepared in DCE at C_{pol} = 5 wt % (δ-form); and subsequently (b) annealed at 130 °C or (c) annealed at 220 °C.

and 20.5° observed after annealing at 220 °C (Figure 1c) show the formation of the α-form,[14] as generally observed for analogous thermal treatments on sPS samples.[15]

In this respect, it is worth adding that, as for δ-form powder and film samples,[12] the DSC traces (not shown here) of δ-form aerogels exhibit an exothermic phase transition at nearly 120 °C corresponding to the recrystallization of the δ-form into the γ-form, followed by another small exothermic peak at 190 °C that is attributed to the $\gamma \rightarrow \alpha$ transition.

The degree of crystallinity for the δ, γ, and α aerogels of Figure 1 is close to 35, 30, and 42%, respectively.

The densities (apparent and skeletal) and the porosity of aerogels obtained by solvent extraction from gels in toluene and DCE (C_{pol} =5 wt %), and then annealed at 130 and 220 °C are reported in Table 1.

Data reported in Table 1 show that the annealing induces a significant decrease of the aerogel porosity that is particularly relevant for the aerogel obtained from the toluene based gel. This lower thermal stability of aerogels from toluene could be possibly explained by smaller crystalline domain size. In fact, as already observed in a recent paper,[16] the correlation lengths of the crystalline domains perpendicular to (010) planes (D_{010}) for δ-form aerogels obtained from toluene gels are smaller than those obtained from DCE gels. In particular, for gels prepared at C_{pol}=5 wt % in DCE and toluene, D_{010} is equal to 10 and 6.5 nm, respectively.

The influence of thermal treatments on aerogel morphology was also investigated and the SEM micrographs of δ-form aerogels obtained from gel prepared in DCE, after annealing at 130 and 220 °C, are reported in Figure 2. For the sake of comparison, the micrograph of the starting δ-form aerogel before annealing is also reported.

The SEM micrographs clearly show that the morphology of γ and α aerogels obtained by annealing is largely different from the morphology of the starting δ-form aerogel. Although the starting aerogel (Figure A) displays a fibrillar morphology with fibril diameters in the range 30−100 nm, after annealing at 130 °C, adjacent fibers have started to weld together and the γ-form aerogel still displays a fiberlike morphology with fibril diameters up to 300 nm. Conversely, after annealing at 220 °C, the fibers have almost totally welded together leading to a continuous skin.

(B) High-Porosity γ- and β-Form Aerogels by High-Temperature Supercritical CO_2 Extraction. Supercritical CO_2 extraction of sPS gels exhibiting a cocrystalline phase allows to obtain high-porosity monolithic aerogels, for broad temperature ranges. For instance, starting from a gel prepared in DCE at C_{pol} = 5 wt %, the obtained aerogels exhibit a porosity of ca. 92%, for the whole considered temperature range (40−150 °C) (see Figure 3 for an aerogel obtained after extraction at 150 °C).

In Figure 4 are reported the X-ray diffraction patterns of aerogels obtained from gels prepared in DCE at C_{pol} = 5 wt %, after supercritical carbon dioxide extraction at (a) 130 and (b) 150 °C.

The X-ray diffraction pattern of the sample obtained after extraction at 130 °C (Figure 4a) displays strong reflections at 2θ = 9.4, 10.4, 16, and 20°, thus indicating the formation of a γ-form[13] aerogel, whereas the reflections at 2θ = 6.1, 10.5, 12.3, 13.5, 18.6, and 20.2° observed for the sample obtained after extraction at 150 °C (Figure 4b) indicate the formation of a β-form[17] aerogel.

In this respect, it is worth citing that it is well-known that treatments by supercritical CO_2 can induce crystal-to-crystal transformations in sPS,[18] and more specifically that high-temperature supercritical CO_2 treatments can induce, in sPS cocrystalline films, transformation of cocrystalline phases into γ- and β-phases.[18d]

It is worth noting that for the β-form aerogel obtained by gel extraction with supercritical CO_2 at 150 °C, both the degree of crystallinity (40%) and the structural order (D_{020}

(12) (a) Manfredi, C.; De Rosa, C.; Guerra, G.; Rapacciuolo, M.; Auriemma, F.; Corradini, P. *Macromol. Chem. Phys.* **1995**, *196*, 2795–2808. (b) Manfredi, C.; Guerra, G.; De Rosa, C.; Busico, V.; Corradini, P. *Macromolecules* **1995**, *28*, 6508–6515. (c) Gowd, E. B.; Shibayama, N.; Tashiro, K. *Macromolecules* **2006**, *39*, 8412–8418.
(13) Rizzo, P.; Lamberti, M.; Albunia, A. R.; Ruiz de Ballesteros, O.; Guerra, G. *Macromolecules* **2002**, *35*, 5854–5860.
(14) (a) De Rosa, C.; Guerra, G.; Petraccone, V.; Corradini, P. *Polym. J.* **1991**, *23*, 1435–1442. (b) Cartier, L.; Okihara, T.; Lotz, B. *Macromolecules* **1998**, *31*, 3303–3310.
(15) (a) Immirzi, A.; de Candia, F.; Iannelli, P.; Zambelli, A.; Vittoria, V. *Makromol. Chem., Rapid Commun.* **1988**, *9*, 761–764. (b) Guerra, G.; Vitagliano, V. M.; De Rosa, C.; Petraccone, V.; Corradini, P. *Macromolecules* **1990**, *23*, 1539–1544. (c) Corradini, P.; Guerra, G. *Adv. Polym. Sci.* **1992**, *100*, 182–217. (d) Chatani, Y.; Shimane, Y.; Inoue, Y.; Inagaki, T.; Ishioka, T.; Ijitsu, T.; Yukinari, T. *Polymer* **1992**, *33*, 488–492. (e) Rizzo, P.; Albunia, A. R.; Guerra, G. *Polymer* **2005**, *46*, 9549. (f) Gowd, E. B.; Shibayama, N.; Tashiro, K. *Macromolecules* **2008**, *41*, 2541–2547.
(16) Daniel, C.; Avallone, A.; Guerra, G. *Macromolecules* **2006**, *30*, 7578–7582.
(17) De Rosa, C.; Rapacciuolo, M.; Guerra, G.; Petraccone, V.; Corradini, P. *Polymer* **1992**, *32*, 1423–1428.
(18) (a) Handa, Y. P.; Zhang, Z.; Wong, B. *Macromolecules* **1997**, *30*, 8499–8504. (b) Reverchon, E.; Guerra, G.; Venditto, V. *J. Appl. Polym. Sci.* **1999**, *74*, 2077–2082. (c) Ma, W.; Yu, J.; He, J. *Macromolecules* **2004**, *37*, 6912–6917. (d) Ma, W.; Yu, J.; He, J. *Macromolecules* **2005**, *38*, 4755–4760. (e) Ma, W.; Andersson, A.; He, J.; Maurer, F. H. J. *Macromolecules* **2008**, *41*, 5307–5312.

Table 1. Porosity *P* (%), Apparent Density ρ_a (g/cm^3), Skeletal Density ρ_s (g/cm^3), and BET (m^2/g) Values of sPS Aerogels Obtained by Annealing or by Supercritical Carbon Dioxide Extraction Procedure

	sPS/DCE (5 wt %)	sPS/toluene (5 wt %)	BET (m^2/g)
δ-form CO_2 extraction at 40 °C	$P = 93$, $\rho_a = 0.07$, $\rho_s = 1.02$	$P = 94$, $\rho_a = 0.05$, $\rho_s = 1.02$	290[a]
γ-form annealing at 130 °C of δ-form aerogel	$P = 65$, $\rho_a = 0.36$, $\rho_s = 1.06$	$P = 17$, $\rho_a = 0.87$, $\rho_s = 1.05$[b]	nd
α-form annealing at 220 °C of δ-form aerogel	$P = 61$, $\rho_a = 0.40$, $\rho_s = 1.04$	$P = 15$, $\rho_a = 0.88$, $\rho_s = 1.04$	nd
γ-form CO_2 extraction at 130 °C	$P = 92$, $\rho_a = 0.09$, $\rho_s = 1.07$	nd	nd
β-form CO_2 extraction at 150 °C	$P = 92$, $\rho_a = 0.08$, $\rho_s = 1.06$	nd	64
ε-form	$P = 89$, $\rho_a = 0.11$, $\rho_s = 1.02$	nd	230

[a] Evaluated for aerogels with a porosity $P = 90\%$ obtained from gels prepared in toluene at $C_{pol} = 10$ wt %.

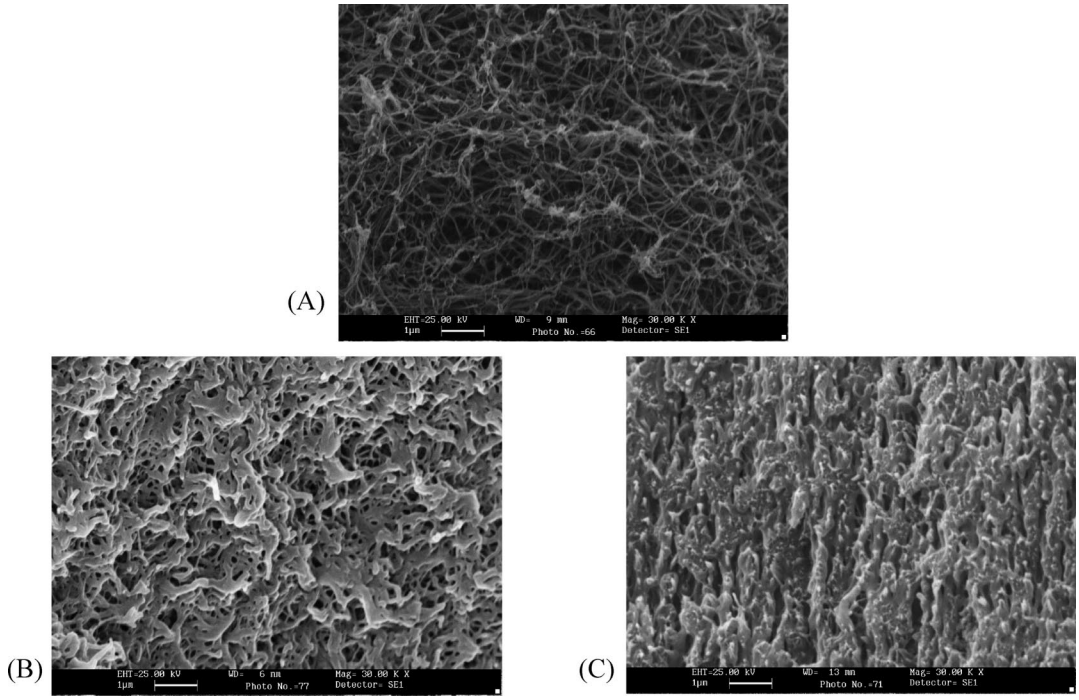

Figure 2. Electron micrographs of δ-form aerogels obtained from gels prepared in DCE at $C_{pol} = 5$ wt % (A) before annealing and after annealing at (B) 130 and (C) 220 °C. Magnification 30 000× for all micrographs; scale as indicated.

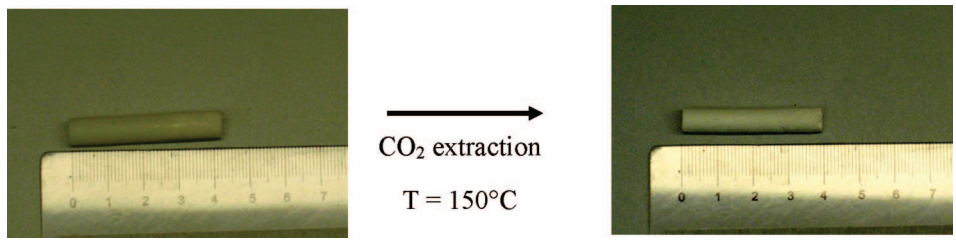

Figure 3. Photographs of a piece of sPS gel prepared in DCE at $C_{pol} = 5$ wt %, before and after complete DCE extraction by supercritical CO_2 extraction at 150 °C.

= 14 nm, corresponding to the diffraction peak located at $2\theta = 6.1°$) are lower than for a β-form aerogel obtained by extraction with supercritical CO_2 at 40 °C of a gel with β-crystalline junctions, whose X-ray diffraction pattern is shown, for example, in Figure 2a of ref 1a (48% and 35 nm, respectively).[1a] On the other hand, for the γ-form aerogel obtained by gel extraction with supercritical CO_2 at 130 °C (Figure 4a), both the degree of crystallinity (40%) and the structural order ($D_{200} = 13$ nm, corresponding to the diffraction peak located at $2\theta = 9.3°$) are larger than for the γ-form aerogel obtained by annealing at 130 °C of a δ-form aerogel (30% and 7 nm, respectively; curve a of Figure 1). The higher degree of crystallinity and crystalline order of γ-form aerogels obtained by extraction at 130 °C can be attributed to a plasticizing effect of supercritical CO_2, which also induces a decrease in the γ-form formation temperature of ca. 20 °C.[18d]

In Figure 5 are reported the SEM micrographs of the γ-form (Figure 5A) and β-form (Figure 5B) high-porosity aerogels obtained after supercritical carbon dioxide extraction at 130 and 150 °C, respectively.

The micrographs clearly show that high temperature surpercritical CO_2 extraction leads to aerogels with a fibrillar morphology with fibril diameters in the range 30−150 nm, similar to those observed for δ-form aerogels.[1] This confirms the hypothesis[1a] that the supercritical carbon dioxide extraction allows us to obtain aerogels where the polymer essentially preserves the morphology occurring in the native gels.

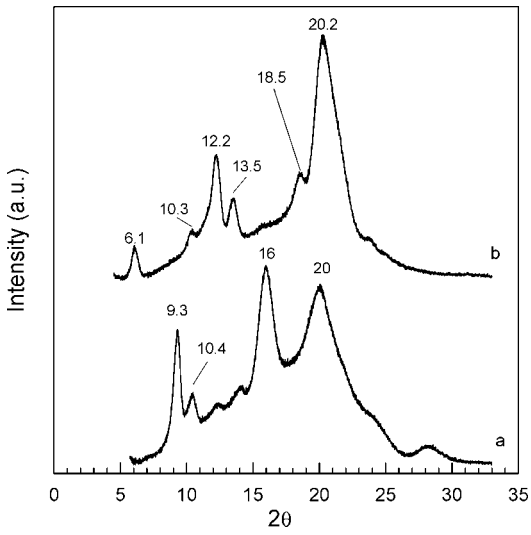

Figure 4. X-ray diffraction patterns of sPS aerogels obtained from gels prepared in DCE at C_{pol} = 5 wt %, after supercritical carbon dioxide extraction at (a) 130 and (b) 150 °C.

It is worth noting that the preparation procedure described in this section allows us to achieve β- and γ-aerogels presenting the same fibrillar morphology of the known δ-form aerogels, whereas in previous reports[1a,b,e] only the achievement of β-form aerogels with lamellar morphology and poor mechanical properties has been described.

It is also worth emphasizing that γ- and β-aerogels having the same fibrillar morphology and the same apparent porosity than δ-form aerogels, are in fact characterized by a much lower surface area. In particular, a β-aerogel with an apparent porosity $P = 92\%$ has a BET = 64 m^2/g, whereas a δ-aerogel with an apparent porosity $P = 90\%$ has a BET = 290 m^2/g. This large difference is of course due to the micropores of the δ-form.

(C) ε-Form Aerogels. The recently reported second nanoporous crystalline phase of sPS, named ε,[8] can be obtained by treatment with liquid chloroform of γ-form samples (film or powder) followed by chloroform removal, by volatile guests of sPS, like acetone or acetonitrile or CO_2.[8]

A high porosity γ-form aerogel ($P = 92\%$), obtained by supercritical carbon dioxide extraction at 130 °C of a sPS/DCE gel and similar to that one of Figure 4a, was immerged in chloroform for 12 h and then extracted by supercritical carbon dioxide at 40 °C.

These two treatments lead to a monolithic aerogel with a porosity $P = 89\%$ (see photographs in Supporting Information), only slightly reduced with respect to the porosity of the starting γ-form aerogel ($P = 92\%$). Typical X-ray diffraction pattern and electron micrograph of the thus obtained aerogel are reported in panels A and B in Figure 6, respectively.

The X-ray diffraction pattern displays strong reflections at $2\theta = 6.9$, 8.1, 13.7, 16.2, 20.5, 23.5, and 28.5° indicating the formation of the ε-form crystalline form,[8] which is characterized by channel-shaped cavities crossing the unit cells along the c axis. The SEM analysis shows that the fibrillar morphology of the starting γ-aerogel (Figure 4A) is substantially modified by the chloroform treatment, so that the obtained ε-aerogel presents a sort of open pore morphology, with pores with diameters in the range 0.5−2 μm. The BET value measured for an ε aerogel with a porosity $P = 89\%$ is 230 m^2/g.

In summary, ε aerogels are characterized by macropores in the range 0.5−2 μm and a polymer framework presenting the channel-shaped microcavities of the crystalline ε-form (as schematically shown in Figure 5C).

(D) Sorption of Organic Molecules from Diluted Aqueous Solutions. Previous studies have shown that small organic pollutants, e.g., 1,2-dichloroethane (DCE),[2c,7b,c,j,11] can easily form cocrystals by sorption (also from very diluted solutions)[7] into δ-form samples, whereas larger molecules,[2e] e.g., 4-(dimethyl-amino)-cinnamaldehyde (DMACA, molecular volume of 0.275 nm^3),[9b] are unsuitable to form a cocrystal structure by sorption into the δ-form. On the other hand, preliminary studies on ε-form films have shown that this microporous phase, due to its channel-shaped (rather than cavity-shaped) porosity, is able to absorb both small molecules like DCE as well as long large-volume molecules like DMACA.

Sorption of organic molecules from dilute aqueous solutions is presently investigated for aerogels of high and similar porosity ($88\% < P < 90\%$) and exhibiting different crystalline phases. In particular, the equilibrium uptake of DCE and DMACA has been measured.

In Figure 7, DCE equilibrium uptakes from diluted aqueous solutions (determined by the intensity of suitable FTIR peaks, as calibrated by thermogravimetric measurements) from ε aerogels ($P = 88\%$) are compared to the equilibrium uptake of γ aerogel ($P = 90\%$) and δ aerogel ($P = 90\%$). For the sake of comparison, equilibrium sorption capacity of DCE from activated carbon is also shown.[19]

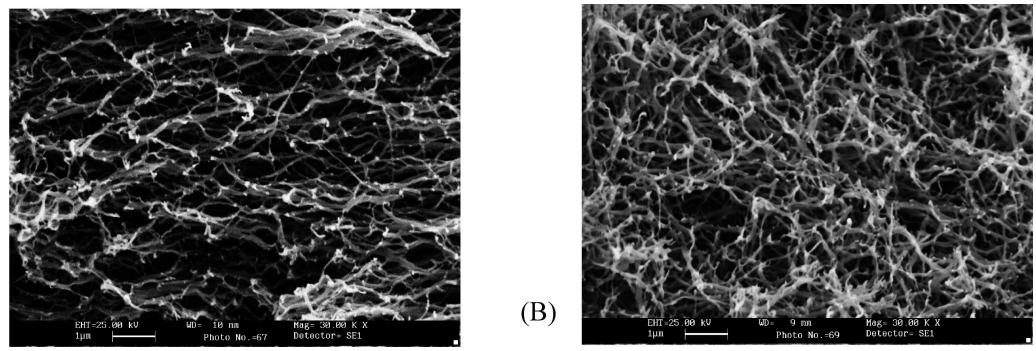

Figure 5. Electron micrographs of (A) γ- and (B) β-form aerogels obtained from gels prepared in DCE at C_{pol} = 5 wt % after supercritical carbon dioxide extraction at 130 and 150 °C. Magnification 30 000× for both micrographs; scale as indicated.

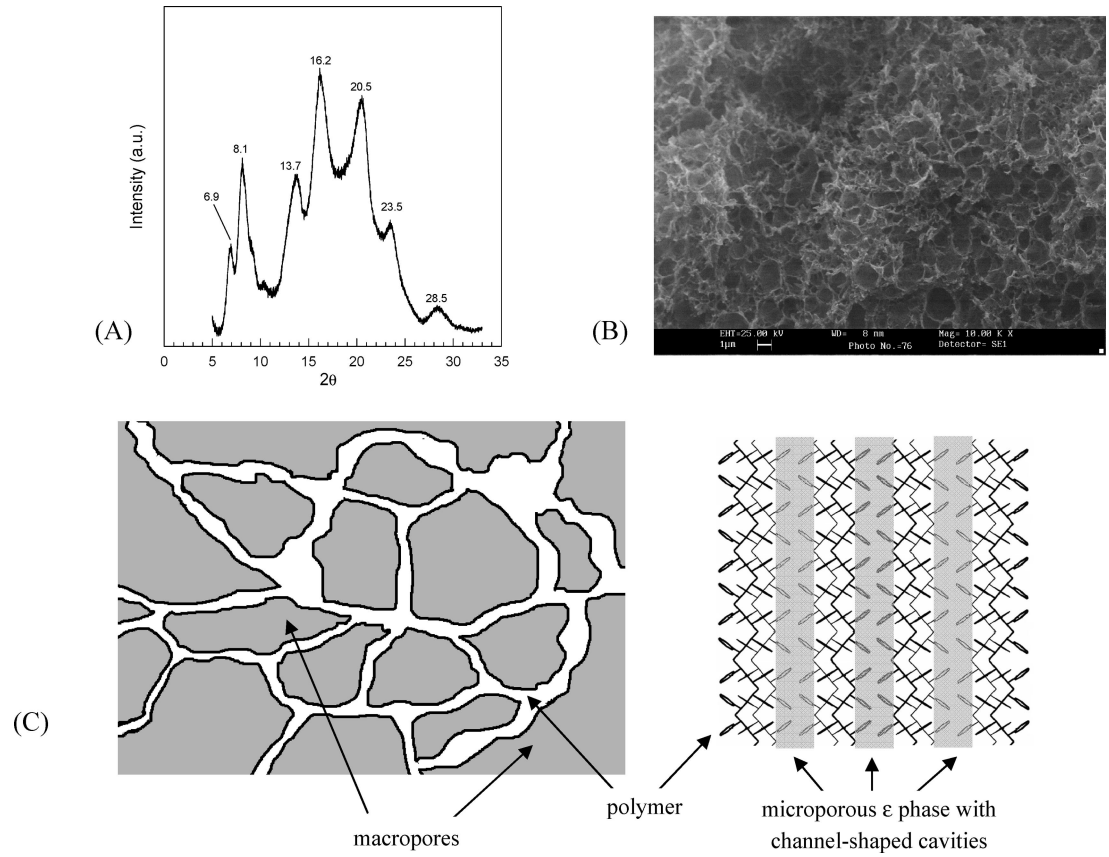

Figure 6. (A) X-ray diffraction pattern and (B) electron micrograph of a sPS aerogel ($P = 89\%$) obtained from a γ-form aerogel ($P = 93\%$), after immersion in chloroform followed by supercritical carbon dioxide extraction at 40 °C. Magnification 10 000× for the micrograph; scale as indicated. (C) Schematic representation of the texture (left) and the microporous crystalline structure (right) of ε-aerogels.

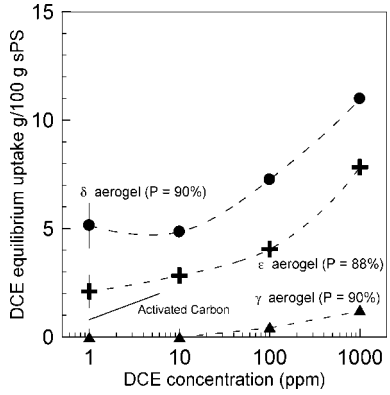

Figure 7. Equilibrium DCE sorption at room temperature by δ aerogel ($P = 90\%$, filled circles, data by Daniel et al.[1e]), ε aerogels ($P = 88\%$, crosses), and γ aerogels ($P = 90\%$, triangles, data by Daniel et al.[1e]) as determined by FTIR measurements. DCE sorption from activated carbon is also reported (thin line, data from M.H Stanzel[19]).

We can observe that the equilibrium DCE uptake from the ε-form aerogel is lower than for the δ-form aerogel but much larger than for the γ-form aerogel. This clearly indicates that the DCE uptake occurs essentially only in the micropores of the δ and ε forms. As a consequence, the equilibrium DCE uptake of aerogels is independent of the apparent porosity, size, and size distribution of the macropores.[1e]

It is also worth noting that the DCE uptake, from highly diluted aqueous solutions, for ε-form aerogels is high (e.g., higher than 2 wt % for 1 ppm of DCE concentration) and also higher than for activated carbons.

The FTIR spectra of a δ-aerogel ($P = 90\%$) and a ε-aerogel ($P = 88\%$) before (curves a and c, respectively) and after equilibrium sorption from a 12 ppm DMACA aqueous solution (curves b and d, respectively), are reported in Figure 8A.

We can observe that for the δ-form aerogel the FTIR spectra before (curve a in Figure 8A) and after immersion in the aqueous solution of DMACA (curve b in Figure 8A) are nearly identical. This indicates that DMACA sorption from the aqueous solution for the aerogel with the nanoporous δ-form is negligible, as for the aerogels with dense crystalline phases (β or γ). Conversely, absorption peaks located at 1674, 1526, 1131, and 1116 cm^{-1} (curve d in Figure 8A) clearly indicate a large uptake of DMACA in the ε-form aerogel. For instance, the DMACA uptake in the ε-form aerogel from 12 ppm aqueous solution is close to 3 wt %, as evaluated on the basis of thermogravimetric measurements (not shown here).

The negligible sorption of the long and bulky guests from β, γ, and δ aerogels having similar porosity and morphology clearly indicates that, for low activity, DMACA molecules are absorbed essentially only in the channel-shaped cavities of the ε-form crystalline phase rather than in the amorphous macropores of the aerogel. The absence of sorption in δ-form aerogels is due to the molecular volume of DMACA molecules which are, unlike DCE, too bulky to enter in the microporous cavities of the δ crystalline phase.

(19) Stanzel, M. H. *Chem. Eng. Progr.* **1993**, *89* (4), 36–43.

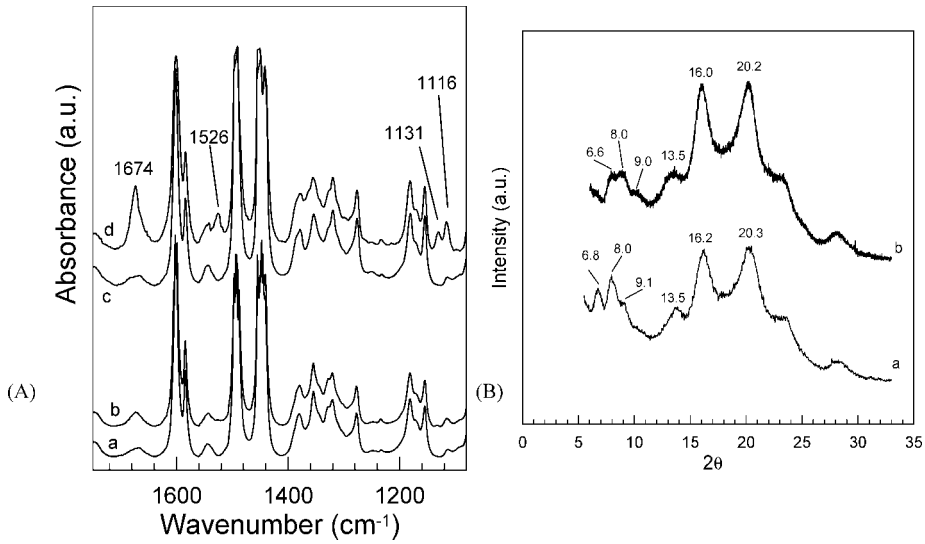

Figure 8. (A) FTIR spectra in the wavenumber range 1080−1750 cm^{-1} for a (a, b) δ-form and (c, d) ε-form aerogel, (a, c) before and (b, d) after equilibrium sorption from a 12 ppm DMACA aqueous solution. (B) X-ray diffraction patterns of a ε-form aerogel (curve a) before and (curve b) after equilibrium sorption from a 12 ppm DMACA aqueous solution.

In Figure 8B are compared the X-ray diffraction patterns of ε-form aerogel before (curve a) and after (curve b) sorption of DMACA from a 12 ppm aqueous solution. We can observe a change of the diffraction pattern with a decrease of the intensity of the diffraction peaks located at $2\theta = 6.8$ and 8.0°. This kind of pattern variation, also observed for sorption of different guests into the nanoporous ε-phase, confirms that DMACA molecules are absorbed in the crystalline phase.

Conclusions

In this paper, the crystalline structure, morphology, and porosity of sPS aerogels obtained by thermal treatments and high-temperature supercritical-CO_2 extractions have been investigated.

Thermal annealing procedures on δ-form aerogels allow the formation of γ- and α-form aerogels, although a significant decrease of the aerogel porosity, associated with substantial morphological changes, is observed. This aerogel shrinkage is less pronounced for δ-form aerogels exhibiting more ordered crystalline junctions (as, for example, those obtained from sPS/DCE gels).

High-temperature supercritical CO_2 extraction procedures, on the other hand, allow obtaining high-porosity monolithic γ and β aerogels. Moreover, these high temperature extractions lead to aerogels with a fibrillar morphology with fibril diameters in the range 30−150 nm, similar to those observed for δ-form aerogels, where the polymer essentially preserves the morphology occurring in the native gels.

Treatments of γ-form aerogels with chloroform, followed by solvent extraction by supercritical CO_2 at 40 °C, can lead to the formation of high porosity monolithic aerogels with the recently discovered nanoporous ε-form.

Sorption of organic molecules from aqueous diluted solutions is high and fast by sPS aerogels, only when a nanoporous crystalline phase (δ or ε) is present. Moreover, the guest uptake depends strongly on the guest molar volume. In particular, the small DCE molecules can be efficiently absorbed by both δ and ε aerogels, although the guest uptake is higher for δ aerogels. Conversely, the DMACA long molecules are efficiently absorbed from diluted aqueous solutions only by the ε aerogel. Of course, for long guests, the channel-shaped cavities of the sPS ε-form play a key role in the aerogel sorption capacity. The reported results clearly indicate that ε-form aerogels are suitable for detection and removal of long organic molecules from water.

Acknowledgment. Financial support of the "Ministero dell'Istruzione, dell'Università e della Ricerca" (PRIN2007) and of Regione Campania (Centro di Competenza) is gratefully acknowledged. Prof. Ernesto Reverchon and dr. Paola Rizzo of University of Salerno are acknowledged for useful discussions. Prof. Giuseppe Mensitieri of University of Naples "Federico II" is acknowledged for having made available microscopy facilities and Prof. Giuseppe Spoto of Turin University is also acknowledged for specific surface area measurements.

Supporting Information Available: Information containing photographs of monolithic γ and ε aerogels (PDF). This material is available free of charge via the Internet at http://pubs.acs.org.

CM802537G